# Kinematic Modeling and Control Algorithm for Non-holonomic Mobile Manipulator and Testing on WMRA system.

Lei Wu, Redwan Alqasemi and Rajiv Dubey

***Abstract*— In this paper, we will explore combining the manipulation of a robotic arm and the mobility of a mobile platform, both in theory and in hardware implementation. First, the kinematic equations of the 7-DoF redundant robotic arm and the 2-DoF non-holonomic mobile platform will be introduced. Second, we will derive the Jacobian equations of the robotic arm and the mobile platform. The two Jacobian equations will be combined into one so we can accomplish the end-effector guided control without the consideration of controlling the mobile platform separately. Finally, we will implement and test these algorithms both on the simulated and physical Wheelchair-Mounted Robotic Arm (WMRA) system. Comparison and analysis of the results will be presented, and future improvements will be discussed.**

***Index Terms*— Jacobians, Kinematics, Mobile manipulator, Non-holonomic system, Redundant robotic arm, Wheelchair Mounted Robotic Arm system(WMRAs).**

## I. INTRODUCTION

The 9-DoF wheelchair-mounted robotic arm (WMRA) system consists of a 2-DoF non-holonomic mobile platform and a 7-DoF redundant robotic arm, see Fig. 1. Applications for this system can be used in assistant wheelchairs for disabilities, industrial mobile manipulators and warehouse storage robots. Unfortunately, most WMRAs have had limited commercial success due to poor usability. It is often difficult to accomplish many of the Activities of Daily Living (ADL) tasks with the WMRAs currently on the market due to their physical and control limitations and its control independence of the wheelchairs' control system.

Fig. 1. Wheelchair-mounted robotic arm system.

Seraji uses the combined Jacobian matrices to solve a simple on-line approach for motion control of holonomic mobile robots [1]. Lim and Seraji presented a real-time system which controls the 7-DoF robotic arm and 1-DoF mobile platform [2]. White evaluated the dynamic redundancy resolution in a non-holonomic wheeled mobile manipulator [3]. Chen presented an adaptive sliding mode backstepping control for the mobile manipulator with non-holonomic constraints [4].

In this paper, we are going to introduce the WMRA system which has the uniqueness in using the universal two wheel driven non-holonomic mobile platform instead of using the omni-directional mobile platform, which has a difficulty overcoming the drifting problem. The uniqueness is the integrated control algorithm of the two systems. We will present how to model the mobile platform in which the arm mounting position is offsetting both in X, Y and Z directions. The combination with the 7-DoF redundant robotic arm will be introduced.

It is desired to fulfill the need of such integrated systems to be used for many ADL tasks, such as opening a spring-loaded door autonomously and go through it, interactively exchange objects with a companion on the move, avoid obstacles by going around them while maneuvering objects, conveniently handle food and beverage between the fridge, Microwave oven, stove, etc. without the need to switch between the wheelchair controller and the robotic arm controller, and avoid singularities in a small working environment, such as an office, where wheelchair motion can be slightly utilized to maneuver objects while avoiding singularities (similar to a person sitting on an office chair and handling objects around him by moving his/her arm while slightly moving the chair to get closer to an object that is otherwise unreachable).

## II. KINEMATIC MODELING OF MOBILE MANIPULATORS

### A. Kinematics of 7-DoF Redundant Robotic Arm

The robotic arm at hand consists of seven revolute joints of which the rotation axes of every two immediate joints intersect. Fig. 2 shows a Solid Works drawing of the new robotic manipulator that was designed and built at the University of South Florida [5]. For that manipulator, frame assignment for each link is shown in Fig. 3, and the D-H parameters are highlighted.

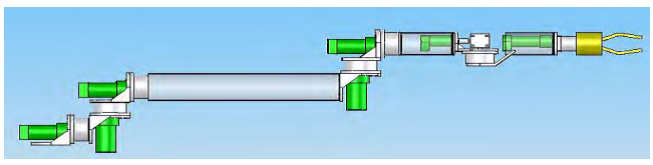

Fig. 2. Solid Works Model of the New 7-DoF Robotic Arm Built at USF.

*1) The Homogeneous Transformation Matrices:* The aim of the forward kinematics is to solve the transformation equations for the end-effector's Cartesian position and orientation or velocities when the joint angles and velocities are

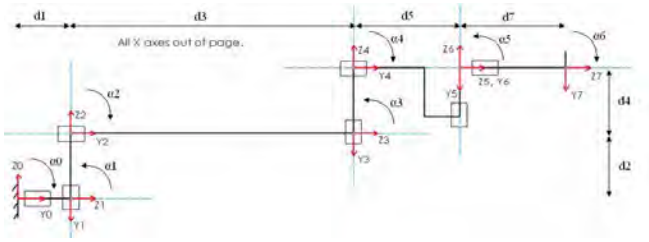


Fig. 3. Frame Assignments and Dimensions of the 7-DoF Robotic Arm.

TABLE I

THE D-H PARAMETERS OF THE 7-DOF ROBOTIC ARM.

| $i$ | $\alpha_{i-1}$ | $a_{i-1}$ | $d_i$ | $\theta_i$ |
|---|---|---|---|---|
| 1 | -90 | 0 | $d_1$ | $\theta_1$ |
| 2 | 90 | 0 | $d_2$ | $\theta_2$ |
| 3 | -90 | 0 | $d_3$ | $\theta_3$ |
| 4 | 90 | 0 | $d_4$ | $\theta_4$ |
| 5 | -90 | 0 | $d_5$ | $\theta_5$ |
| 6 | 90 | 0 | $d_6$ | $\theta_6$ |
| 7 | -90 | 0 | $d_7$ | $\theta_7$ |

given. Homogeneous transformation matrices that transform the motion from one coordinate frame reference to the other can be easily obtained from the D-H parameters using the conventional equations [6] that relate every two consecutive frames to each other as follows:

$$ {}^{i+1}_{i}T = \begin{bmatrix} C\theta_i & -S\theta_i & 0 & a_{i-1} \\ S\theta_i \cdot C\alpha_{i-1} & C\theta_i \cdot C\alpha_{i-1} & -S\alpha_{i-1} & -S\alpha_{i-1} \cdot d_i \\ S\theta_i \cdot C\alpha_{i-1} & C\theta_i \cdot S\alpha_{i-1} & C\alpha_{i-1} & C\alpha_{i-1} \cdot d_i \\ 0 & 0 & 0 & 1 \end{bmatrix} \quad (1) $$

Where $S$ is sine, and $C$ is cosine of the angle. Propagating these matrices from one frame to the other gives us the forward kinematics of the robotic arm that describes the end-effector's frame based on the base frame as follows:

$$ {}^{Armbase}_{End-effector}T = {}^{A}_{E}T = {}^{0}_{1}T \cdot {}^{1}_{2}T \cdot {}^{2}_{3}T \cdot {}^{3}_{4}T \cdot {}^{4}_{5}T \cdot {}^{5}_{6}T \cdot {}^{6}_{7}T \quad (2) $$

*2) The Jacobian Matrices:* We can compute the manipulator Jacobian matrix by simply doing some manipulation of Transformation matrix ${}^{A}_{E}T$. Detailed steps please reference Orin and Schrader's efficient computation of the Jacobian matrix for robot manipulator [7].

$$ \dot{X}_E^{w.r.tA} = J_E \cdot \dot{q}_A \quad (3) $$

Where $J_E$ is the Jacobian matrix that relates the 7 joint angular velocities to the end-effector's Cartesian velocities based on the arm base frame. At any time step, knowing the joint velocities and joint angles allows us to translate directly to the end-effector's Cartesian velocities using the Jacobian matrix. $\dot{X}_E^{w.r.tA}$ is the velocities of end-effector in Cartesian space with respect to arm base frame.

### B. Kinematics of 2-DoF Mobile Platform

If the controllable DoF is less than the total DoF in the workspace, then the platform is said to be non-holonomic [8]. Examples of non-holonomic platforms are cars, power wheelchairs and other mobile platforms that can, at any given moment, move in two dimensions out of the three planar dimensions. The wheelchair used in this work is an "Action Ranger X Storm Series" power wheelchair. This wheelchair accomplishes its non-holonomic motion using a differential drive that carries two independently-driven wheels in the back of the power wheelchair. The front of the wheelchair has two passive castors that are placed to support the wheelchair's motion. This makes the wheelchair a 2-DoF system that moves in plane [9].

Three important points of interest were assigned on and around this wheelchair, and coordinate frames were assigned on these three points. These three frames are the wheelchair's coordinate frame assigned at the center of the driving wheels' axle, the ground frame assigned at an arbitrary location on the ground floor, and another frame called frame "$A$" assigned at the point where the 7-DoF robotic arm will be mounted. Fig. 4 shows two-dimensional top and side views of the SolidWorks model of the wheelchair with the key dimensions and the frame assignments.

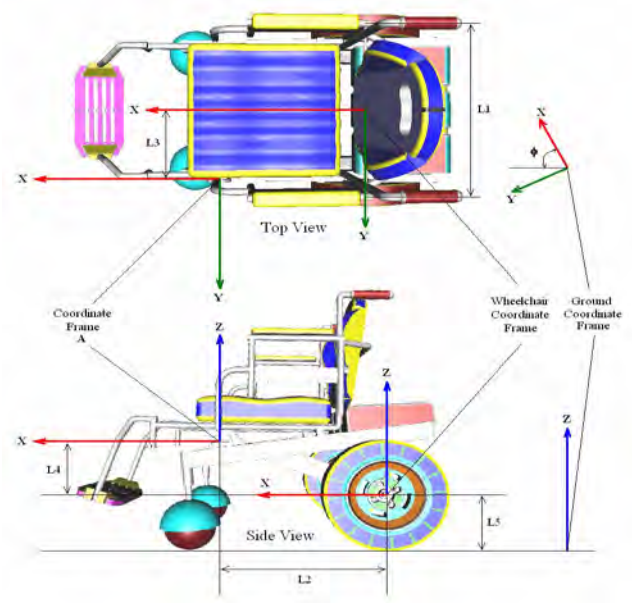


Fig. 4. Mobile platform coordinate frames and dimensions of interest.

Where $L_1$ is the distance between the centers of the two driving wheels along the differential drive axle, $L_2$ $L_3$ $L_4$ are the offset distances from the center of the differential drive to the center of frame "$A$" along the wheelchair's X-axis, Y-axis and Z-axis respectively. And the $L_5$ is the offset distance from the center of the differential drive to the center of the ground frame along the wheelchair's Z-axis, which is the same as the wheelchair's driving wheels' radius.

*1) The Homogeneous Transformation Matrices:* To transform the wheelchair's coordinate frame during motion, we assume that the initial position and orientation of the frame is known, and we need to find the new position and orientation for the next time step. Let the initial coordinate frame of the wheelchair be "$W_0$" and the next coordinate frame after moving one step is "$W_1$" as shown in Fig. 5.

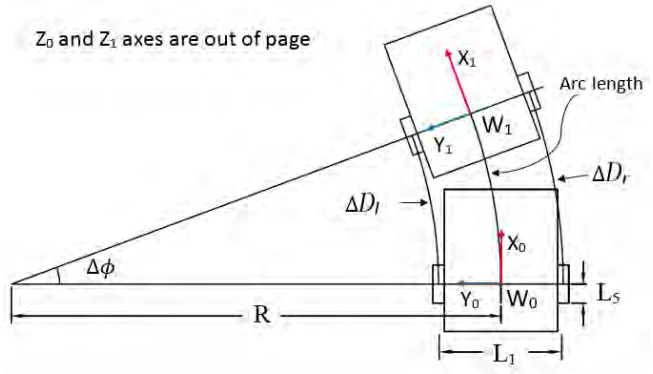


Fig. 5. Transformation of mobile platform frames.

$$\text{Arc length} = \frac{\Delta D_l + \Delta D_r}{2} \tag{4}$$

$$\Delta\phi = \frac{\Delta D_r - \Delta D_l}{L_1} \tag{5}$$

$$R = \frac{\text{Arc length}}{\Delta\phi} \tag{6}$$

Where $\Delta D_l = L_5 \cdot d\theta_l$, $\Delta D_r = L_5 \cdot d\theta_r$. $L_5$ is the radius of the wheel. $d\theta_l$ and $d\theta_l$ are the rotational changes during this time loop which can be obtained from the motor encoders. So the transformation from the known coordinate "$W_0$" to the next time step "$W_1$" would be:

$$^{W_0}_{W_1}T = \begin{bmatrix} C\Delta\phi & -S\Delta\phi & 0 & R\cdot S\Delta\phi \\ S\Delta\phi & C\Delta\phi & 0 & R - R\cdot C\Delta\phi \\ 0 & 0 & 1 & 0 \\ 0 & 0 & 0 & 1 \end{bmatrix} \tag{7}$$

For the purpose of the robotic arm to be mounted on the wheelchair, one more transformation is required between the wheelchair's coordinate frame and the robotic arm base coordinate frame where it attaches to the wheelchair.

$$^{W_1}_{A}T = \begin{bmatrix} 1 & 0 & 0 & L_2 \\ 0 & 1 & 0 & L_3 \\ 0 & 0 & 1 & L_4 \\ 0 & 0 & 0 & 1 \end{bmatrix} \tag{8}$$

If we assume that the initial coordinate frame of the wheelchair "$W_0$" was a result of previous transformation from the origin "$G$" as illustrated in Fig. 4, the resulting homogeneous transformation from the ground frame "$G$" to the wheelchair's initial frame "$W_0$" can be expressed as:

$$^{G}_{W_0}T = \begin{bmatrix} C\phi & -S\phi & 0 & P_{0x} \\ S\phi & C\phi & 0 & P_{0y} \\ 0 & 0 & 1 & L_5 \\ 0 & 0 & 0 & 1 \end{bmatrix} \tag{9}$$

Where $\phi$ is the resultant turning angle from all previous steps added together. The origion of $W_0$ coordinate indicated by $P_{0x}$ and $P_{0y}$ are the resultant positions from all previous steps added together in global X and Y axes respectively .

Multiplying (9) (7) and (8) together results in the relation between the ground coordinate frame "$G$" and the final coordinate frame of the wheelchair "$A$" as follows:

$$^{G}_{A}T = {}^{G}_{W_0}T \cdot {}^{W_0}_{W_1}T \cdot {}^{W_1}_{A}T \tag{10}$$

*2) The General Jabocian Matrices:* We can compute the mobile base Jacobian by using velocity propagation approach. For detailed steps please reference Alqasemi's maximizing manipulation capabilities of persons with disabilities [10].

$$V_A = J_{whA} \cdot \dot{q}_{wh}, \text{ or} \tag{11}$$

$$\begin{bmatrix} \dot{X}_A \\ \dot{Y}_A \\ \dot{\phi}_A \end{bmatrix} = \frac{L_5}{2} \begin{bmatrix} C\phi + \frac{2}{L_1}(L_2 S\phi + L_3 C\phi) & C\phi - \frac{2}{L_1}(L_2 S\phi + L_3 C\phi) \\ S\phi - \frac{2}{L_1}(L_2 C\phi - L_3 S\phi) & S\phi + \frac{2}{L_1}(L_2 C\phi - L_3 S\phi) \\ -\frac{2}{L_1} & \frac{2}{L_1} \end{bmatrix} \begin{bmatrix} \dot{\theta}_l \\ \dot{\theta}_r \end{bmatrix} \tag{12}$$

Where $J_{whA}$ is the Jacobian matrix that relates the wheels' angular velocities to the arm base or arm mounting place Cartesian velocities with respect to the global frame "G".

The above equation will be used with the numerical methods to produce the motion commanded by the user in Cartesian coordinates after calculating the wheels' velocities required to realize the commanded motion. And it is a universal Jacobian matrix that can be used in any 2-DoF non-holonomic mobile system. For example, some platforms' arm mounting place has no offset in X-axis; therefore, we just need simply let $L_2$ =0.

### C. Kinematics of Integrated Mobile Manipulator

*1) The Homogeneous Transformation Matrices:*

$$^{G}_{E}T = {}^{G}_{A}T \cdot {}^{A}_{E}T \tag{13}$$

Matrix $^{G}_{E}T$ represents the 4×4 homogeneous transformation between the ground and the end-effector's frame in terms of the WMRA joint space.

*2) The Jacobian Matrices:* In order to combine the motion of the arm with the motion of the wheelchair, it is important to modify the Jacobian matrix of wheelchair to include all six Cartesian velocities in space. So the (12) should be rewritten as:

$$V_A{}^{6D} = J_{whA}{}^{6D} \cdot \dot{q}_{wh}, \text{ or} \tag{14}$$

$$\begin{bmatrix} \dot{X} \\ \dot{Y} \\ \dot{Z} \\ \omega_x \\ \omega_y \\ \omega_z \end{bmatrix}_A = \frac{L_5}{2} \begin{bmatrix} C\phi + \frac{2}{L_1}(L_2 S\phi + L_3 C\phi) & C\phi - \frac{2}{L_1}(L_2 S\phi + L_3 C\phi) \\ S\phi - \frac{2}{L_1}(L_2 C\phi - L_3 S\phi) & S\phi + \frac{2}{L_1}(L_2 C\phi - L_3 S\phi) \\ 0 & 0 \\ 0 & 0 \\ 0 & 0 \\ -\frac{2}{L_1} & \frac{2}{L_1} \end{bmatrix} \begin{bmatrix} \dot{\theta}_l \\ \dot{\theta}_r \end{bmatrix} \tag{15}$$

Note that the Jacobian equation in (15) relates the wheels' velocity vector to the Cartesian task space at the robotic arm base frame, and what we need is the equivalent relationship defined at the end-effector's frame. This will be done to the wheelchair's motion by introducing a new Jacobian as follows:

$$J_A^E = \begin{bmatrix} I_2 & [0] & -(P_{Ex}\cdot S\phi + P_{Ey}\cdot C\phi) \\ [0] & & P_{Ex}\cdot C\phi - P_{Ey}\cdot S\phi \\ & & I_4 \end{bmatrix} \tag{16}$$

Where $P_{Ex}$ and $P_{Ey}$ are the x-y coordinates of the end-effector based on the arm base frame which can be obtained from the transformation matrix ${}^{A}_{E}T$.

It is important to keep all the Jacobian matrices with respect to the global coordinate "G", so the Jacobian matrix in the (20) should be rewritten as:

$$J_E{}^G = {}^{G}_{A}R_{6\times 6} \cdot J_E \text{ , or} \tag{17}$$

$$J_E{}^G = \begin{bmatrix} {}^{G}_{A}R & [0] \\ [0] & {}^{G}_{A}R \end{bmatrix} \cdot J_E \tag{18}$$

Where the ${}^{G}_{A}R$ is the 3×3 rotation matrix which can be obtained from ${}^{G}_{A}T$.

Now the Jacobian equations are augmented separately and ready for combination.

$$\dot{X}_E^{w.r.tG} = J_E{}^G \cdot \dot{q}_A + J_A^E \cdot J_{whA}{}^{6D} \cdot \dot{q}_{wh} \text{ , or} \tag{19}$$

$$\begin{bmatrix} \dot{X} \\ \dot{Y} \\ \dot{Z} \\ \omega_x \\ \omega_y \\ \omega_z \end{bmatrix}_E = \begin{bmatrix} J_E{}^G & J_A^E \cdot J_{whA}{}^{6D} \end{bmatrix}_{6\times 9} \cdot \begin{bmatrix} \dot{\theta}_1 \\ \dot{\theta}_2 \\ \dot{\theta}_3 \\ \dot{\theta}_4 \\ \dot{\theta}_5 \\ \dot{\theta}_6 \\ \dot{\theta}_7 \\ \dot{\theta}_l \\ \dot{\theta}_r \end{bmatrix}_{9\times 1} \text{ , or} \tag{20}$$

$$\dot{X}_E^{w.r.tG} = J_G^E \cdot \dot{q} \tag{21}$$

where $J_G^E = \begin{bmatrix} J_E{}^G & J_A^E \cdot J_{whA}{}^{6D} \end{bmatrix}$, which is the final combined Jacobian matrix that relates all the 9 joint angular velocities to the end-effector's Cartesian velocities based on the global frame "G".

## III. Hardware Implementation

### A. Hardware design

For the mobile platform, we modified a universal motor powered wheelchair. The arm mounting system was added to the left side of the wheelchair, and the controller box was added to the back side of the wheelchair. The two motors of the wheelchair were modified with two 1000 pulses/revolution incremental encoders, see Fig.6. We chose

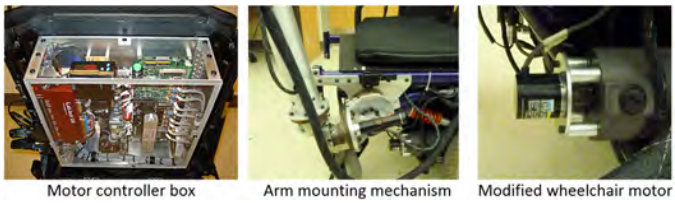


Fig. 6. Important hardware parts.

the Galil DMC-41x3 series motor controller to drive these two wheels, which allows for 4-axis 750W drives, since each motor of the wheelchair has a typical power consumption of 350W. The control board interfaces to a PC with Ethernet 10/100BASE-T which supports TCP/IP or UDP for communication. For the robotic arm, which has 7 servo motor driven joints, each motor was equipped with incremental encoder. The controller is Galil DMC-21x3 series, which allows 8-axis 500W drives in total. The controller board interfaces to a PC with Ethernet 10Base-T which supports TCP/IP or UDP for communication.

### B. Software structure

The communication between Matlab program and the Galil controller board was designed to use Matlab socket(TCP/IP). All algorithms were programmed in the Matlab environment, where the output of the program is the velocity vector of the 9 joints which are sent to the Galil board at each loop. The input of this program is a vector of the current joint angles read from the Galil motor controller at each loop in encoder counts. Fig.7 shows a flowchart of the algorithm to help with understanding how these equations and variables are used in the actual program.

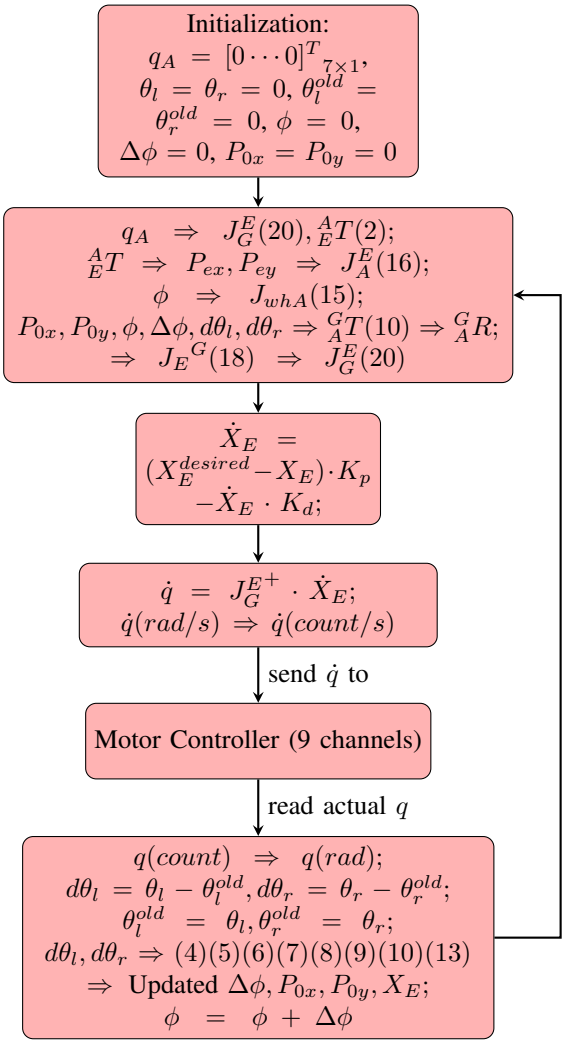


Fig. 7. Control flow diagram.

## IV. Experiment and Results

We designed two tests to verify this algorithm. The first one is commanding the end-effector to follow a straight path at a certain speed. The second one is commanding the end-effector to follow a sinusoidal trajectory.

In the first test, the desired end-effector's trajectory was generated as a linear trajectory as follows:

$$X_E^{desired} = \begin{bmatrix} 90t \\ 0 \\ 0 \\ 0 \\ 0 \\ 0 \end{bmatrix} + X_E^{Initial}$$

where $X_E^{Initial}$ is the initial position(in mm) and orientation(in rad) of the end-effector.

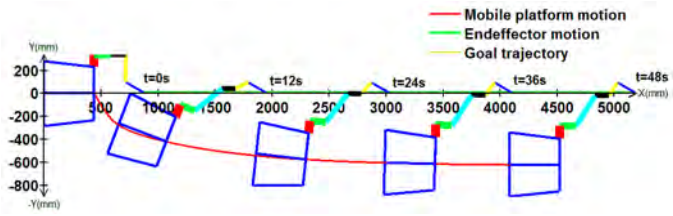


Fig. 8. Following the straight trajectory.

The end-effector's trajectory for the second test was generated as a sinusoidal trajectory as follows:

$$X_E^{desired} = \begin{bmatrix} 90 \cdot t \\ 1000 \cdot \sin(0.1 \cdot t) \\ 0 \\ 0 \\ 0 \\ 0 \end{bmatrix} + X_E^{Initial}$$

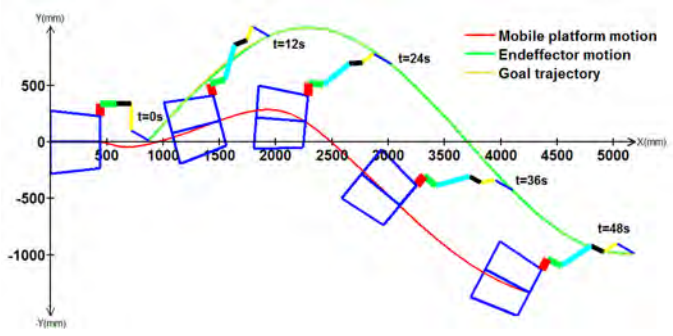


Fig. 9. Following the sinusoidal trajectory.

Fig. 8 and Fig. 9 present the real-time plotting of the operation of the mobile manipulator. The collected data from the 9 encoders based on the feedback from the controller board in real-time(around 100Hz) were used in Matlab algorithm to generate the motion of the physical hardware, as presented in Fig. 8 and Fig. 9. Then the data was sent to the forward kinematic equations to get the Cartesian positions and orientations of each joint (for detailed steps please see Fig. 7).

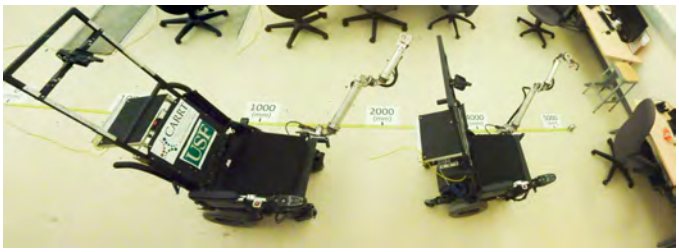


Fig. 10. Panorama picture of test 1 (Top view).

Fig. 10 shows a panoramic view of the test setup from the top view of the first test. We can see a tape measure in the image, which plays the role of the end-effector's trajectory. The landmarks(0mm, 1000mm,...,5000mm) in the picture represent the ticks of the trajectory. This setup will help with verifying that the Matlab algorithm is correctly plotting the position of the mobile robot in the real world.

## V. CONCLUSIONS

In this paper, we presented a generalized mobile manipulator system which includes a 2-DoF non-holonomic mobile platform and a 7-DoF redundant robotic manipulator. The arm mounting position is offsetting from the center of the driving shaft in X,Y and Z axes. So, the kinematic and Jacobian equations derived here are universal form that can be applied to any situation of non-holonomic mobile platforms. We first introduced the kinematic and Jacobian equations of the manipulator and the mobile platform independently, then we adjusted the Jacobian equation of the robotic arm so that the motion of the end-effector will be relative to global frame. Finally, the two Jacobian equations were combined into one; by this way, the end-effector of the mobile manipulator can be easily navigated by the trajectory generated in the global frame. In the hardware testing, the control diagram was introduced in order to give detailed programming steps so that people can easily repeat this experiment. We verified this algorithm on the Wheelchair mounted robotic arm system(WMRAs) built at USF. From the two experiments, we can see that the mobile manipulator can be used to follow the user commanded trajectories. The kinematics modeling is valid and the control algorithm is correct. This algorithm is applicable for any end-effector based application. For example, surface processing (sanding, coating removal, or painting) of large systems such as aircraft or ships.

## VI. FUTURE WORK

Since the mobile platform trajectory is undefined and unknown when the program is running, this may not be desirable for operating in a constrained space. Thus, we are going to introduce a safety motion band for the mobile platform in order to limit the mobile platform moving from the outside of a specific area(safety band) while keeping the end-effector following its own trajectory. The differences between

assigning a specific trajectory for the mobile platform and the safety band concept are as follows:

- Generating the trajectory for mobile platform may not be necessary, since the mobile platform usually has its own safety working range. We can free the motion of the mobile platform as long as it remains in its safety working range.
- Freeing the mobile platform motion instead of keeping specific trajectory will produce more redundancy(usually 2-DoF) for the whole system, so we can use this extra redundancy to optimize algorithms, such as maximizing manipulability of the robotic arm on the mobile manipulator or avoiding the joint limits.

## REFERENCES


[1] H. Seraji, "A unified approach to motion control of mobile manipulators," *The International Journal of Robotics Research*, vol. 17, no. 2, pp. 107–118, 1998.

[2] D. Lim and H. Seraji, "Configuration control of a mobile dexterous robot: Real-time implementation and experimentation," *The International Journal of Robotics Research*, vol. 16, no. 5, pp. 601–618, 1997.

[3] G. White, R. Bhatt, C. P. Tang, and V. Krovi, "Experimental evaluation of dynamic redundancy resolution in a nonholonomic wheeled mobile manipulator," *Mechatronics, IEEE/ASME Transactions on*, vol. 14, pp. 349–357, June 2009.

[4] N. Chen, F. Song, G. Li, X. Sun, and C. Ai, "An adaptive sliding mode backstepping control for the mobile manipulator with nonholonomic constraints," *Communications in Nonlinear Science and Numerical Simulation*, vol. 18, no. 10, pp. 2885 – 2899, 2013.

[5] K. Edwards, R. Alqasemi, and R. Dubey, "Design, construction and testing of a wheelchair-mounted robotic arm," in *Robotics and Automation, 2006. ICRA 2006. Proceedings 2006 IEEE International Conference on*, pp. 3165–3170, May 2006.

[6] J. Craig, *Introduction to robotics: mechanics and control*, vol. 3. Addison- Wesley Publishing, 2003.

[7] D. E. Orin and W. W. Schrader, "Efficient computation of the jacobian for robot manipulators," *The International Journal of Robotics Research*, vol. 3, no. 4, pp. 66–75, 1984.

[8] O. Krupkov and P. Voln, "Eulerlagrange and hamilton equations for non-holonomic systems in field theory," *Journal of Physics A: Mathematical and General*, vol. 38, no. 40, p. 8715, 2005.

[9] E. Papadopoulos and J. Poulakakis, "Planning and model-based control for mobile manipulators," in *Intelligent Robots and Systems, 2000. (IROS 2000). Proceedings. 2000 IEEE/RSJ International Conference on*, vol. 3, pp. 1810–1815 vol.3, 2000.

[10] R. M. Alqasemi, *Maximizing manipulation capabilities of persons with disabilities using a smart 9-degree-of-freedom wheelchair-mounted robotic arm system*. PhD thesis, University of South Florida, 2007.